Available online at www.sciencedirect.com
SCIENCE DIRECT®
International Journal of Heat and Mass Transfer 48 (2005) 3793–3803
International Journal of HEAT and MASS TRANSFER
www.elsevier.com/locate/ijhmt

Metal foam heat sink for transmission window

G. Hetsroni *, M. Gurevich, R. Rozenblit

Department of Mechanical Engineering, Technion, Israel Institute of Technology, 32000 Haifa, Israel

Received 8 December 2004

Abstract

A cooling device for transmission window of an accelerator based on aluminum foam with an inner heat production was investigated experimentally. Dissipation of heat flux up to 0.25 kW/cm^2 was obtained, by using porous metal with porosity of 40 pores per inch. Under these conditions, the difference between the temperatures of the wall and the bulk water did not exceed 45 K and the pressure difference per unit length was 20 bar/m. Image processing of thermal maps of the surface of the metal foam showed that boundary conditions with constant heat flux became more relevant for numerical model than those with constant temperature at high values of Reynolds numbers Re_K based on the permeability.

Keywords: Heat transfer; Metal foam; Transmission window; Enhancement; Drag reduction

1. Introduction

Forced convection in porous media has been studied extensively [1] for over 50 years. However, most studies were restricted to packed beds and granular materials, since they have direct application to naturally occurring porous media, with porosities in the range 0.4–0.6. There are relatively few investigations of transport phenomena in very high porosity media $\varepsilon \approx 0.9$, such as metal foams. Hunt and Tien [2] studied forced convection in metal foams with water as the fluid phase. Using the technique of volume averaging, and under the simplifying assumption of local thermal equilibrium, they showed that a single energy equation could adequately describe forced convection in metal foams. Only during the last 10 years, transport phenomena in metal foams began to receive attention [3–7]. Lee et al. [3] studied the application of metal foams as high-performance air-cooled heat sinks in electronics packaging. In their experimental study, they demonstrated that a 1 cm^2 chip, dissipating 100 W, could be cooled by using an aluminum foam heat sink, and a low-power fan. Recently, Calmidi and Mahajan [4] addressed heat conduction in aluminum metal foams. They obtained experimental data and developed an analytical model for the thermal conductivity, taking into account the open-celled structure of the metal foams. Bhattacharya et al. [5] extended that work to cover a wider range of solid to fluid conductivity ratios. Metal foams can be broadly classified as porous media in which the medium has a distinct but continuous and rigid solid phase, and a fluid phase. They are typically available in high porosities. The foams also have a unique open-celled structure. As a result, most of the past studies on packed beds, and granular porous media are not applicable to metal foams. A

* Corresponding author. Tel.: +972 48 292058; fax: +972 48 238101.
E-mail address: hetsroni@tx.technion.ac.il (G. Hetsroni).

0017-9310/$ - see front matter © 2005 Elsevier Ltd. All rights reserved.
doi:10.1016/j.ijheatmasstransfer.2005.02.040

Nomenclature

C_p	specific heat
D	hydraulic diameter
h	heat transfer coefficient
I_C	inertial coefficient
K	permeability
$\dot{m}$	flow rate
P	energy
q	heat flux
T	temperature
t	foil thickness
S	area
U	average liquid velocity
W	power
y	coordinate perpendicularly to the foil

Greek symbols

ε	porosity
κ	thermal conductivity
v	kinematic viscosity
ρ	density
σ_{SB}	Stefan–Boltzmann constant

Subscripts

a	ambient
f	fluid
fill	filled
in	inlet
out	outlet
s	solid
w	wall

detailed study of forced convection in metal foams has been performed by Calmidi and Mahajan, [6]. The goal of the study was to quantify thermal dispersion and thermal nonequilibrium effects in metal foams. To this end, both experimental and numerical methods were employed. Experiments were performed with a wide variety of aluminum metal foams. Results indicate that for foam-air combinations, the transport enhancing effect of thermal dispersion is extremely low due to the relatively high conductivity of the solid matrix. However, for foam-water combinations results indicate that thermal dispersion can be very high and accounts for the bulk of the transport. Boomsma et al. [7] considered open-cell metal foam as cooling media for compact heat exchangers. They showed that compressed aluminum foam had thermal resistance half to a third lower than currently used exchangers, designed for the same application, while requiring the same pumping power.

The high performance of metal foam heat sinks shows considerable promise as a means for cooling the windows for a transmission of high-energy beams [8] from a high vacuum to atmospheric pressure. The beam energy heats the window, reduces its mechanical strength, and thus limits the particles flux through the window.

The most effective way of cooling the transmission window is by pumping liquid inside the window membrane through micro-channels or porous medium. However, cooling of these devices need an additional examination because of the heat release in the inner volume of the porous membrane when transmitting particle beam.

The aim of this research is to study experimentally the effect of internal heat release on the heat transfer and to formulate a model for numerical simulation of the boundary conditions on the surface of porous materials.

2. Problem description and modeling

A thin foil window (Fig. 1a) is usually used to divide the vacuum space, where the high-energy particle beam is accelerated, from the atmospheric conditions, where it could be applied for irradiation of surfaces, impact ionization, medical equipment sterilization, material joining and cutting etc. The specific power P absorbed by the transmission window depends on the kind of particle beam, the foil thickness t and the material. This energy is linearly proportional to the foil thickness and inversely proportional to the kinetic energy of the beam [9]. Minimal foil thickness is determined by the strength adequate to withstand the pressure difference at maximal working temperature.

The energy P absorbed by the foil is dissipated by three mechanisms

$$P = P_{\text{conv}} + P_{\text{rad}} + P_{\text{cond}} \tag{1}$$

Here P_{conv}, P_{rad}, P_{cond} are heat losses by convection, radiation and conduction, respectively.

The value of losses by convection from the outer surfaces of the window to ambient is estimated as

$$P_{\text{conv}} = h_{\text{conv}}(\overline{T}_{\text{w}} - T_{\text{a}})S \tag{2}$$

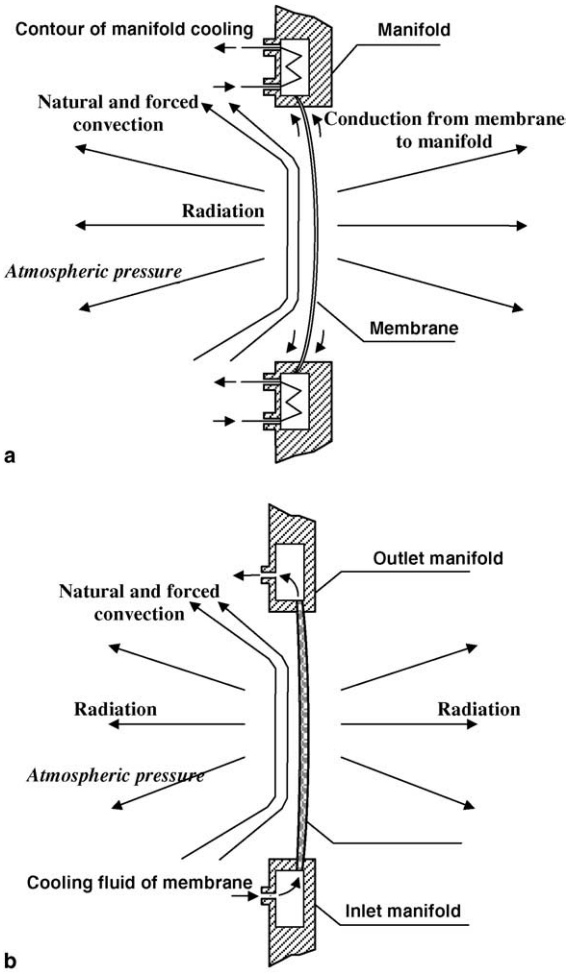

Fig. 1. Schematic diagram of the transmission window: (a) usual cooling and (b) forced cooling using porous media.

where h_{conv} is convective heat transfer coefficient, S is the one side of the surface of the foil, $\overline{T}_w$ is the average temperature of the foil window, T_a is the ambient temperature.

The second mode is radiation from both sides of the foil

$$P_{rad} = 2\sigma_{SB}\varepsilon_w S(\overline{T}_w^4 - T_a^4), \tag{3}$$

here σ_{SB} is the Stefan–Boltzmann constant and ε_w is the foil surface emissivity.

The value of losses by conduction through the foil material to the heat sink on the window periphery may be estimated [9] as

$$P_{cond} = 4\pi kt(T_c - T_p) \tag{4}$$

where k is the thermal conductivity of the foil material, t is the foil thickness, T_{wc} and T_{wp} are the temperatures of the window center and the foil periphery, respectively.

If the particle beam has relatively little energy, an acceptable thermal regime of the transmission window may be stabilized by convection, radiation and conduction through the window material to the heat sink on the foil frame. Usually, a dissipation of the heat by convection and radiation are less significant compared to conduction. In the case of thin metal foil, we can neglect the temperature distribution perpendicularly to the foil, which is due to the heat generated.

The problem of cooling the window becomes much more complicated when high-energy beams have to be transmitted. It is clear that increasing the thickness of the foil helps to enhance heat transfer by conduction, but on the other hand an increase in the foil thickness results in an increase in the heat generated due to the transmission of the particle beam. The solution of the window cooling problem should be considered in a drastic increase in convection. We have cited results of studies where heat transfer at forced convection was many times enhanced by using porous material.

Consider the simple thermal model (Fig. 1b) of a transmission window with porous material between two very thin metal foils. The cooling fluid is pumped in a channel of width W and thickness of 2δ. The high power particle-beam produces heat in the porous material which acts as a volumetric heat source q_v. Assume that

- the natural convection and radiative heat transfer in the porous material are negligible;
- the flow in the channel is fully developed;
- thermo-physical properties do not depend of the temperature.

Based on these assumptions, the following set of governing equations is obtained [10]:

Solid phase

$$\frac{\partial^2 T_s}{\partial y^2} + \frac{q_v}{\kappa_s} - \frac{h_i S}{\kappa_s}(T_s - T_f) = 0 \tag{5}$$

Liquid phase

$$\frac{\partial^2 T_f}{\partial y^2} + \frac{h_i S}{\kappa_f}(T_s - T_f) = \rho_f c_f u \frac{\partial T_f}{\partial x} \tag{6}$$

where κ_s and κ_f are the effective solid and fluid thermal conductivity, respectively; T_s and T_f are the solid and fluid temperatures; h_i is the interstitial heat transfer coefficient, u is the fluid velocity, ρ_f is the fluid density, c_f is the specific heat of the fluid, and S is the interfacial area per unit volume of the porous medium.

The Brinkman momentum equation for the fully developed flow is

$$\frac{\partial^2 u}{\partial y^2} - \frac{u}{K} - \frac{1}{\mu}\frac{\partial p}{\partial x} = 0 \tag{7}$$

where K is the permeability, μ is the viscosity and p is the pressure inside of the porous layer.

The boundary conditions are:

The fluid velocity on the walls is zero

$$u|_{y=\delta} = 0 \quad \text{and} \quad u|_{y=-\delta} = 0; \tag{8}$$

The boundary condition at the center of the porous layer is

$$\left.\frac{dT_s}{dy}\right|_{y=0} = 0; \quad \left.\frac{dT_f}{dy}\right|_{y=0} = 0; \tag{9}$$

The temperature of the liquid at the entrance to the porous layer is T_{f0}.

Some problems arise in the formulation of the thermal boundary conditions at the wall, which affect the results of the calculations of Eqs. (5)–(7). Reasonable assumptions are needed to obtain correct results. For the case of constant wall heat flux there are four different assumptions [11] or the treatment methods for the boundary conditions of the energy equations. The main difference between them is whether the fluid temperature is equal to the solid-phase temperature on the wall. Lee and Vafai [10], Petersen and Chang [12] and Martin et al. [13] assumed that the fluid temperature was equal to the temperature of the solid on the wall for constant heat flux boundary conditions. For example the boundary condition at $y = \delta$ is

$$T_f|_{y=\delta} \cong T_s|_{y=\delta} \cong T_w \tag{10}$$

In the latter study this assumption was explained by attaching some substrate of high thermal conductivity to the porous wall.

On the other hand, Amiri et al. [14] and Jiang et al. [15] showed that boundary conditions assuming that the heat flux transferred by the solid-phase was equal to that transferred by the fluid gave results of numerical calculations, which agreed well with experimental data.

$$-\kappa_s \left.\frac{dT_s}{dy}\right|_{y=\delta} = -\kappa_f \left.\frac{dT_f}{dy}\right|_{y=\delta} = q_w \tag{11}$$

Amiri et al. [14] noted also that there was a second approach, assuming that each elementary volume (which contains both fluid and solid phases) at the wall surface received a prescribed heat flux that was equal to the wall heat flux. In this case we should consider an energy balance at the interface.

$$\kappa_s \frac{dT_s}{dy} + \kappa_f \left.\frac{dT_f}{dy}\right|_{y=\delta} = q_w \tag{12}$$

Such uncertainty in the definition of thermal boundary condition demands new experimental data. We study experimentally the heat transfer in a porous layer and determine the surface temperature distribution on its outer side.

3. Experimental apparatus and procedure

3.1. Experimental apparatus

The test loop is depicted schematically in Fig. 2. Thoroughly filtered water was used in it as the coolant. The water was supplied to the test section from the entrance tank (1) by a regulated gear pump (2). The rectangular channel of cross-section 10×2 mm and the length of 54 mm was milled on the top of the housing (3). The porous insert (4), of width 10 mm, length 54 mm and of 2 mm thickness was placed in the channel, occupying the entire cross-section. Two temperature measurements ports (5) were bored in the top (9) of the test section. The inlet and outlet temperatures of the working fluid on both sides of the tested part of porous layer of 34 mm length were measured with 0.3 mm type T electrical isolated thermocouples inserted in holes of 2.5 mm diameter drilled in the porous strip. The pressure drop between the inlet and the outlet of test section was measured by a pressure transducer (6). The upper side of the insert was coated by black mat paint of about 20 μm thickness to equalize the emissivity of the aluminum alloy and water on the surface. The inner heat generation was simulated by supplying D.C. power up to 400 A to the foam sample through copper rods, (10). The heater could supply power up to 1.0 kW. The Joule heating is considered as volume averaged and uniformly distributed in the inner volume of porous foam. The change of electrical resistance, because the temperature distribution in the cross-section, is negligible. The thermal field of the upper side of the porous strip was measured by high speed IR camera (7) through IR transmitted glass (8) of 3 mm thickness made of Zinc Sulphide ZnS (Multispectral), with transmission range from 0.37 to 13.5 μm. Microscopic lenses of the camera made it possible to reach the spatial resolution of 15 μm. The water flow rate was measured by a weighing method using the exit tank (11) placed on an electronic scale (12). The experiments were carried out at constant heat flux.

3.2. Test samples

Aluminum foam was used as a porous medium in the model of the heat sink with inner heat generation. The open-cell metal foam has a good effective thermal conductivity and a high value of specific solid–fluid interfacial surface area. A simple estimation [1] of the effective thermal conductivity of a porous media filled with fluid can be made by accounting for the volume fraction of each component:

$$k_{eff} = \varepsilon k_f + (1 - \varepsilon) k_s \tag{13}$$

where ε is the porosity of the material, k_f and k_s are thermal conductivities of the fluid and the solid phases, respectively.

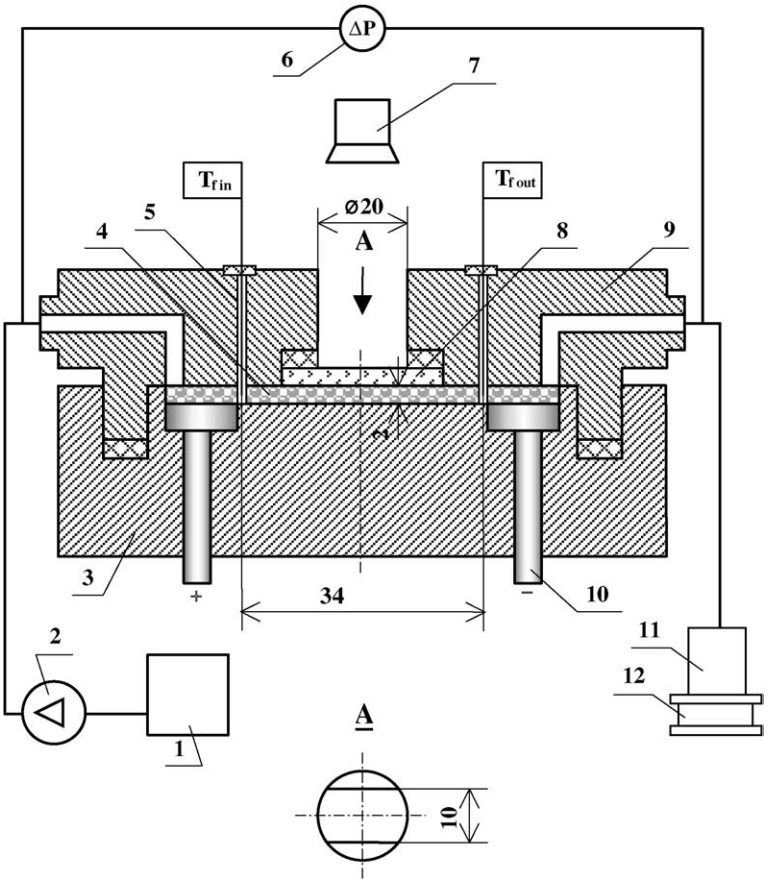

Fig. 2. Experimental facility: (1) entrance tank; (2) pump; (3) housing, (4) sample of porous medium; (5) temperature measurements ports; (6) differential pressure sensor; (7) IR camera; (8) IR transmitted glass; (9) top of test section; (10) two copper rods; (11) exit tank and (12) electronic scales.

Depending on the metal foam configuration, its specific surface area varies from 500 for the original metal foam to 10,000 m^2/m^3 for compressed foam. Aluminum foam of 40 pores per inch (ppi) was studied. The real average pore diameter [7] is about 2.3 mm. The structure of the porous material is presented in Fig. 3.

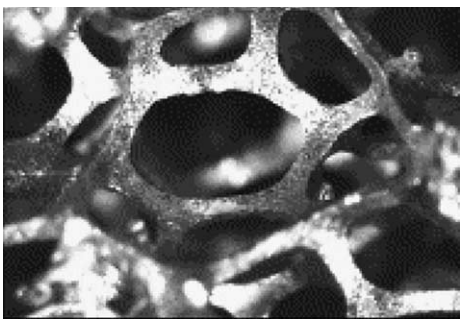

Fig. 3. Sample of aluminum foam. Real size is 3.0×2.2 mm.

The porosity of porous material was calculated by weighing it and comparing the density to that of solid 6101-T6 aluminum alloy. Table 1 lists the corresponding flow properties of the porous aluminum samples.

3.3. Procedure

All measurements were performed under steady state conditions. Each experiment was run for several minutes until the fluid and thermal regimes inside of the porous layer became stabilized. The experiments were carried out in the range of average liquid velocity $0.1 \leqslant U \leqslant 1.2$ m/s in the channel with the porous insert. The range of heat flux was $0.02 \leqslant q \leqslant 0.25$ kW/cm^2. Under these experimental conditions the Reynolds number $Re = \frac{UD}{\nu}$ (D is the hydraulic diameter of the channel; ν is the kinematic viscosity) varied in the range $200 \leqslant Re \leqslant 3800$. The combination of values of the heat flux and velocity was varied in such a way that single-phase fluid flowed in the test section.

Table 1
Aluminum foam properties

Foam ppi	Specific surface area, m^2/m^3	Porosity %	Permeability, $K \times 10^{10}$, m^2	Inertial coefficient I_C
40	2700	85.0	23.4	0.060

Notes: Values of specific surface are according to data cited in Boomsma et al. [7]. Data on the magnitude of the porosity, permeability and inertial coefficient were measured on the samples of aluminum foam supplied by M-PORE GmbH. The foam samples in the channel were slightly (1–3 vol%) pressed, to prevent any water leakage, so the results should be considered as a reference.

According to the definition of the problem, as cooling of the transmission window, the membrane is heated by the particle beam passing through the side surface. Therefore we consider definition of an effective (or conditional) heat flux q as

$$q = \frac{\dot{m} C_p (T_{f,out} - T_{f,in})}{S} \tag{14}$$

where $\dot{m}$ is the flow rate, C_p is the specific heat, $T_{f,in}$ and $T_{f,out}$ are the inlet and the outlet temperatures of the liquid in the channel, S is the side area of the window.

The conditional average heat transfer coefficient is defined as

$$h = \frac{q}{(\overline{T}_W - \overline{T}_f)} \tag{15}$$

where $\overline{T}_W$ is the average wall temperature measured by the IR camera, $\overline{T}_f$ is the average value of the fluid temperature, calculated as the mean of the inlet $T_{f,in}$ and the outlet, $T_{f,out}$, temperatures of the liquid in the test section. All thermophysical parameters of the water, needed for evaluation of the heat transfer coefficient and Reynolds numbers, were determined at the same temperature $\overline{T}_f$.

The IR Radiometer was situated at a distance of about 0.1 m from the IR window of the experimental setup.

3.4. Experimental uncertainty

The flow rate of the water $\dot{m}$ was controlled by adjusting the voltage to the gear pump and was measured by a weighing method with an uncertainty of ±0.2%. The pressure drop between the inlet and the outlet of the test section was measured by means of a pressure transducer with an uncertainty of 1.5%. The data were collected by a 12-bit 1 MHz acquisition system with an uncertainty of ±0.025% FS. The pressure drop measurements were performed both with and without the thermocouples inserted through the ports in the channel, in order to determine their effect on the measurements. The analysis showed that the pressure readings in the both cases were within the uncertainty.

The inlet and outlet temperatures of the working fluid were measured by 0.3 mm type T thermocouples. These thermocouples were calibrated in a narrow temperature range of 25–40 °C with an uncertainty of 0.1 K. The temperature field of the heated surface was measured by the IR camera. The IR camera was calibrated by measuring the temperatures of water preheated before the test section inlet in the range of 20–70 °C. The estimated uncertainty of temperature measurement by IR camera was within 0.3 K at the experimental conditions. In order to calculate the deviations associated with the measurement of various quantities, readings were taken for a few runs every 2 min over a period of 20 min. The error in determining the conditional average heat transfer coefficient h, according to Eqs. (14) and (15), is composed from an estimation of errors of measurements of the follow values: $\dot{m}$ is the mass flow rate; $T_{f,out} - T_{f,in}$ is the difference between outlet and inlet temperatures of the liquid; $\overline{T}_w - \overline{T}_f$ is the difference between the averaged value of the wall and the liquid temperatures. The uncertainty is higher at the higher values of flow rate due to the small temperature difference between the outlet and inlet water temperatures. Therefore, an uncertainty estimation of heat transfer coefficient is done at the highest value of flow rate. The uncertainty of these components (Table 2) for an estimation of an error measurement of heat transfer coefficient was obtained according to the standard 1995 Guide to the Expression of Uncertainty of the Measurements [16]. The uncertainties in determining a thermal conductivity of the cooling water and hydraulic diameter are estimated as 0.4% and 1.2%, respectively. Therefore, the uncertainties of the values of heat transfer coefficient h (Table 2) and the conditional Nusselt number $Nu = hD/k_f$ are within 12.5% and 12.7%, respectively.

4. Results and discussion

4.1. Pressure drop

A series of experiments were performed on the test section with a porous material made of aluminum foam. The pressure difference produced by the porous insert ΔP was computed by subtracting the pressure drop ΔP_{clear} of the channel without the insert from the pressure drop ΔP_{fill} of the channel with porous insert

$$\Delta P = \Delta P_{fill} - \Delta P_{clear} \tag{16}$$

The experimental value of the Darcy velocity was computed for each pressure drop by dividing the flow

Table 2
Summary of standard uncertainty components of heat transfer coefficient ($\dot{m} = 20 \times 10^{-3}$ kg s^{-1})

Standard uncertainty component $u(x_i)$	Source of uncertainty	Value of standard uncertainty $u(x_i)$	$c_i \equiv \partial h/\partial x_i$	$\frac{u(x_i)\lvert c_i\rvert}{h}$
$u(\dot{m})$	Flow rate	2.2×10^{-6} kg/s	$1.23 \times 10^7 \frac{T_{f,out} - T_{f,in}}{\overline{T}_{w,IR} - \overline{T}_f}$	3.73×10^{-4}
$u(T_{f,out} - T_{f,in})$	Measured difference between inlet and outlet liquid temperatures	0.14 K	$1.23 \times 10^7 \frac{\dot{m}}{\overline{T}_{w,IR} - \overline{T}_f}$	5.15×10^{-2}
$u(T_{W,IR} - T_f)$	Measured difference between the wall and the liquid temperatures	0.32 K	$1.23 \times 10^7 \frac{\dot{m}(T_{f,out} - T_{f,in})}{(\overline{T}_{w,IR} - \overline{T}_f)^2}$	2.67×10^{-2}

$u_c(h)/h = 5.88 \times 10^{-2}$; $h = 1.65 \times 10^4$ W/m^{2}K; degrees of freedom—8; $v_{eff}(h) = 15$; $k = 2.13$; $U_{95} = k\ u_c(h)$; $U_{95}(h)/h = 0.125$.

rate $\dot{m}$ by the cross-section area of the channel S_c and liquid density ρ

$$U = \dot{m}/\rho S_c \tag{17}$$

The modified Darcy equation (5) was used to determine the permeability, K, and inertial coefficient, I_C, for each sample

$$\frac{\Delta P}{L} = \frac{\mu}{K} U + \rho \frac{I_C}{\sqrt{K}} U^2 \tag{18}$$

where μ and ρ are dynamic viscosity and density of fluid, respectively.

Fig. 4 shows the pressure drops per the unit length for the porous insert. These data are in good agreement with similar data on pressure drops in [7].

The permeability and inertial coefficient for each porous layer were obtained directly from fitting [17] by quadratic polynomial. Their magnitudes have been listed in Table 1. The data on inertial coefficient were related to the results of study by Bhattacharya et al. [18] who defined the properties of high porosity metal foams. The inertial coefficient in this study is ranged from the value of 0.068 to 0.104 for foam porosity from 0.899 to 0.972. That is why the value of inertial coefficient of 0.06 at porosity of 0.85 in our case may be considered as reasonable.

4.2. Heat transfer

The value of the heat transfer coefficient was determined from Eqs. (14) and (15). Fig. 5 shows the relation between the Nu number $Nu = \frac{hD}{k_f}$ (where h is the conditional heat transfer coefficient; D is the hydraulic diameter of the channel; k_f is the thermal conductivity of the fluid) and the Reynolds number $Re = \frac{UD}{v}$ (where U is the liquid velocity; D is the hydraulic diameter of the channel; v is the kinematic viscosity of the coolant). The dashed line on the bottom of this graph is the theoretical calculation for a channel without porous medium. Simple calculation shows that a dissipation of heat flux up to 0.24 kW/cm^2 was obtained experimentally for Reynolds number value of $Re = 3800$ with a difference between the temperatures of the wall and that of the water of 45 K. Such an increase in the magnitude of heat transfer is achieved by an insignificant increase in the pressure drop per the unit length (Fig. 4) up to 20 bar/m (about 0.8 bar for our setup).

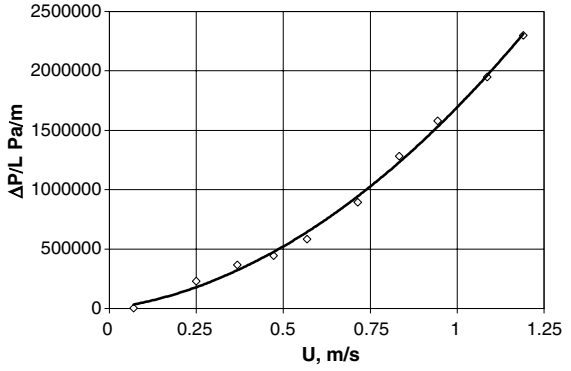

Fig. 4. Pressure drop per the unit length of porous insert vs. Darcy flow velocity.

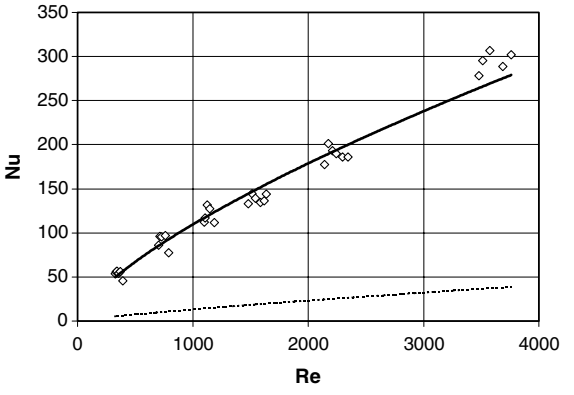

Fig. 5. The relation between the conditional Nusselt and the Reynolds numbers based on hydraulic diameter. The dashed line is the calculation for the clear channel according to equation $Nu = 0.023\, Re^{0.8}\, Pr^{0.4}$.

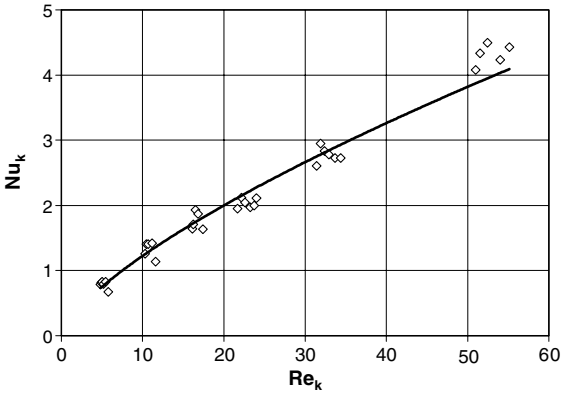

Fig. 6. The relation between the conditional Nusselt, Nu_K and Reynolds, Re_K numbers, based on the permeability value.

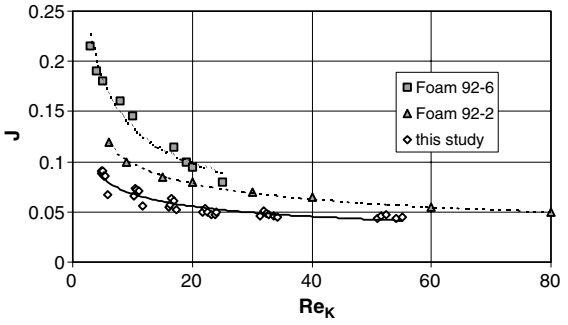

Fig. 7. Colburn j-factor depending on the Reynolds number Re_K based on permeability.

To compare our data on the conditional heat transfer in porous medium with those that could be found in the literature, we should apply dimensionless numbers based on the the properties of the porous material, such as the effective characteristic size $\sqrt{K}$ determined from the data on permeability.

The experimental data on the heat transfer in porous medium is presented as a relation between the Reynolds number $Re_K = \frac{U\sqrt{K}}{\nu}$ and Nusselt number $Nu_K = \frac{h\sqrt{K}}{k_f}$ in Fig. 6. Such presentation makes it possible to generalize the data and estimate the heat transfer characteristics of porous cooling in the channel of different hydraulic diameter filled with porous material.

4.3. Heat sink performance

Now we can compare the efficiency of using aluminum foam for cooling devices with inner heat release with the efficiency of such modern porous media as aluminum compressed foams [7].

A heat sink performance is characterized by the j-Colburn factor:

$$j = St\,Pr^{2/3} \tag{19}$$

where $St = \frac{Nu}{Re\,Pr}$ is the Stanton number and Pr is the Prandtl number. This factor gives the ratio of the convection heat transfer to the required flow rate in the heat sink for different coolants. However since heat conduction perpendicularly the boundary layer has a profound impact on the heat transfer in the metal foam, the magnitude of j-Colburn factor becomes just some measure of heat sink performance. Fig. 7 shows the value of the Colburn factor depending on the Reynolds number $Re_K = \frac{U\sqrt{K}}{\nu}$ for the channel with different aluminum inserts. The values of j-Colburn factor are highest at low values of Reynolds number Re_K.

It is of interest to compare the performance of this heat sink with one of modern high-efficiency heat exchanger [7] on the basis of compressed aluminum foam. The original open-cell foam has porosity of about 92% with an average cell diameter of 2.3 mm. We used for comparison their experimental data for two kinds of aluminum foam with compression ratio of 2 and 6 and measured porosity of about 87% and 67%, respectively. The magnitudes of the Colburn factor j for samples of compressed foams are presented also in the Fig. 7. This graph clearly demonstrates that some compression of the aluminum foam is the right way for the augmentation of heat sink performance for the low values of the Reynolds number. Decrease in the slope and equalization of the j-value at high enough Reynolds numbers Re_K for different kinds of metal foam means that the performance of heat sink decreased and its value becomes independent of the compression ratio.

4.4. Image processing

In order to understand the influence of surface porosity at the boundary of the porous layer on the local heat transfer, one should process the data from a very complicated picture resulting from the fluid motions near the wall and the temperature rise along (from the left to the right) the picture because of the fluid heating. In order to overcome this problem and obtain physically meaningful results, we use a procedure based on averaging of the temperature profiles at ten cross-sections along the flow direction. Mean temperature and standard deviation for each profile were determined.

The data from the IR radiometer were stored in a digital mode. For every set of flow and heat flux conditions the thermal fields of the surface were recorded. An example of temperature distribution of the surface of the porous material is presented in Fig. 8. The thermal maps were then analyzed using the image-processing software. The software makes it possible to establish a temperature profile along any line, determine the mean temperature and the standard deviation (STD). IR image of the

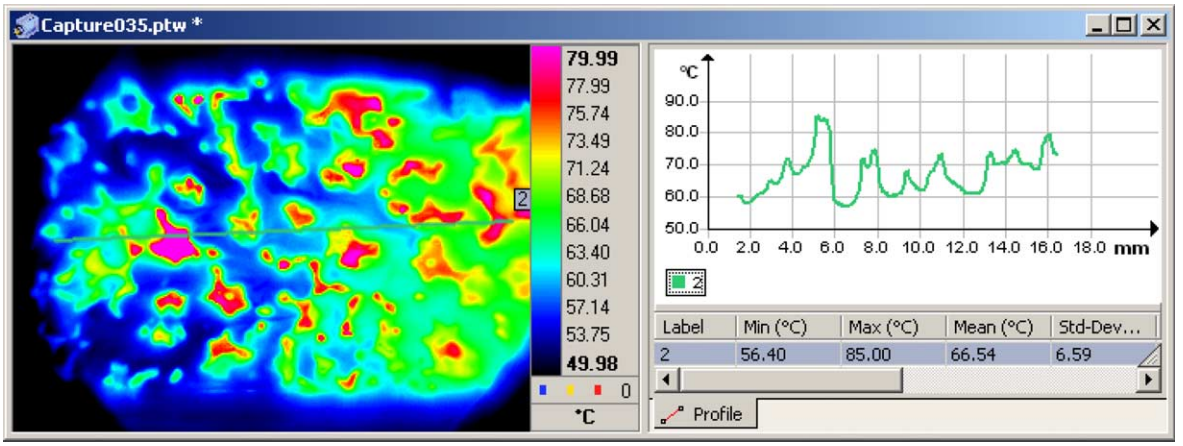

Fig. 8. Typical IR image of the foam surface and temperature profile along of flow direction (Re = 3750, q = 230 W/cm^2).

porous surface shows an increase in the temperature of the window along the flow direction (from left to right). Non-uniformity of the thermal field of the porous layer is determined also by the profile of the flow velocity. The disturbances of the temperature field on the porous sample surface introduced by the influx of the cold fluid from the main stream towards the wall also lead to some changes of uniformity of the thermal field. The size and configuration of these domains depend (at fixed parameters of channel flow) on the velocity and heat flux.

Fig. 9 shows the change of the temperature difference ΔT_w on the sample surface depending on the temperature difference ΔT_f between the outlet and the inlet water temperatures. It can be seen that the value of ΔT_w is proportional to the magnitude of ΔT_f at high enough heat fluxes.

Image processing makes it possible to estimate the effect of an influx of bulk water to the surface of porous sample on the surface temperature distribution introducing special parameter $\frac{\mathrm{STD}(T_w)}{(T_w - T_f)}$ (where $\mathrm{STD}(T_w)$ is the standard deviation of the surface temperature, $(T_w - T_f)$ is the difference between the surface and mean liquid temperatures). In Fig. 10 we can see that the magnitude of this parameter increases with an increase in the value of Re_K (in other words the increase in the cooling velocity or the pore diameter) for low Reynolds numbers. After $Re_K \geqslant 20$ the value of parameter $\frac{\mathrm{STD}(T_w)}{(T_w - T_f)}$ is stabilized on the level of about 0.085–0.09. It means that the temperature differences between the solid and liquid phases at the boundary may be neglected only at very low value of Reynolds number Re_K based on the permeability. In this case, the boundary condition of the $T_f|_{y=\delta} \cong T_s|_{y=\delta} \cong T_w$ may be acceptable. Boundary conditions with constant heat flux become more relevant than those with constant wall temperature at high values of Reynolds numbers Re_K for applications of the metal foam as a cooling medium.

Results of image processing may be presented also in the form (Fig. 11) of the relation of spatial variations of heat transfer on the surface of the porous media $\frac{\mathrm{STD}(T_w)}{(T_w - T_f)} Nu_K$ depending on Reynolds number Re_K. We

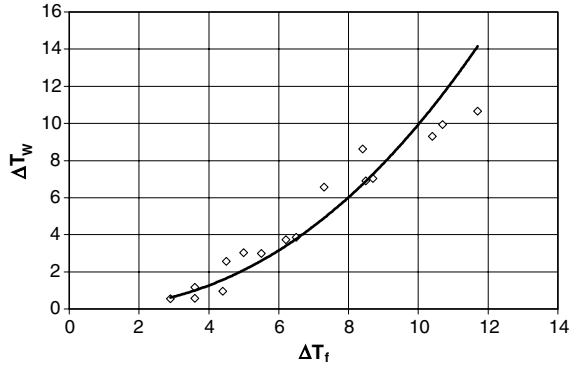

Fig. 9. Temperature difference on the sample surface depending on the difference between outlet and inlet water temperatures.

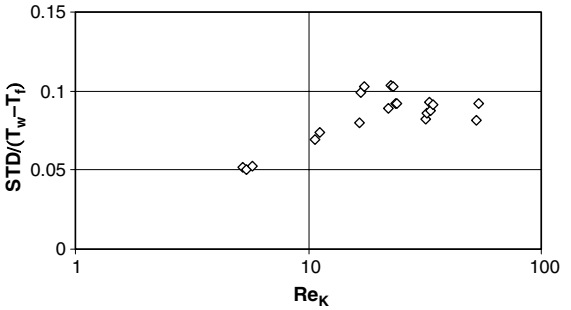

Fig. 10. The effect of an influx of bulk water to the surface of porous sample on the surface temperature distribution.

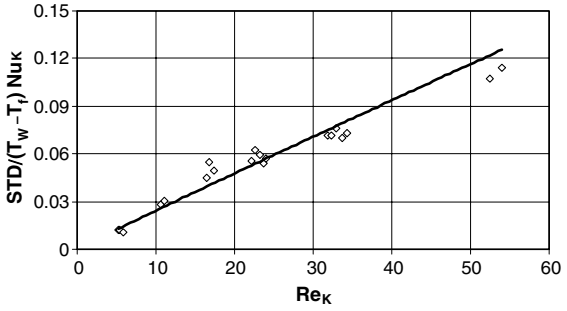

Fig. 11. The relation of spatial variations of heat transfer on the surface of the porous media $\frac{\mathrm{STD}(T_w)}{(T_w - T_f)} Nu_K$ depending on Reynolds number Re_K.

can see that the value of this parameter is continuously increased with increase in Re_K, having the small magnitude at the low Reynolds numbers only.

5. Conclusion

1. A metal foam heat sink for transmission windows with inner heat generation was constructed and investigated experimentally.
2. Dissipation of heat flux up to 0.25 kW/cm^2 was obtained experimentally by using porous samples with porosity 40 pores per inch. Under these experimental conditions, the temperature difference between the temperatures of the wall and the bulk water did not exceed 45 K and the pressure difference per the unit length was 20 bar/m.
3. Image processing of thermal maps on the surface of the metal foam shows that boundary conditions with constant heat flux become more relevant for numerical model than those with constant temperature at high values of Reynolds numbers Re_K, based on the permeability.
4. An estimation of performance of metal foam heat sinks clearly demonstrate the potential of using porous foam for cooling the transmission window with internal heat generation.

Acknowledgement

This research was supported by the Council for Higher Education and by the IAEA Soreq. R. Rozenblit was supported by a joint grant from the Center for Absorption in Science of the Ministry of Immigrant Absorption and the Committee for Planning and Budgeting of the Council for Higher Education under the framework of the KAMEA program. The foam samples, provided by Dr. D. Girlich at M-PORE GmbH, are acknowledged and appreciated.

References

[1] M. Kaviany, Principles of Heat Transfer in Porous Media, second ed., Springer-Verlag, New York, 1995.
[2] M.L. Hunt, C.L. Tien, Effects of thermal dispersion on forced convection in fibrous media, Int. J. Heat Mass Transfer 31 (1988) 301–309.
[3] Y.C. Lee, W. Zhang, H. Xie, R.L. Mahajan, Cooling of a FCHIP Package with 100 W, 1 cm^2 chip, in: Proceedings of the 1993 ASME International Electronic Packaging Conference, vol. 1, ASME, New York, 1993, pp. 419–423.
[4] V.V. Calmidi, R.L. Mahajan, The effective thermal conductivity of high porosity fibrous metal foams, J. Heat Transfer 121 (1999) 466–471.
[5] A. Bhattacharya, V.V. Calmidi, R.L. Mahajan, An analytical–experimental study for the determination of the effective thermal conductivity of high-porosity fibrous foams, in: Proceedings of the ASME IMECE'99, ASME, NewYork, 1999, pp. 13–20.
[6] V.V. Calmidi, R.L. Mahajan, Forced convection in high porosity metal foams, J. Heat Transfer 122 (2000) 557–564.
[7] K. Boomsma, D. Poulikakos, F. Zwick, Metal foams as compact high performance heat exchangers, Mech. Mater. 35 (2003) 1161–1176.
[8] R.J. Vidmar, R.J. Barker, Microchannel cooling for high-energy particle transmission window, an RF transmission window, and VLSI heat dissipation, IEEE Trans. Plasma Sci. 26 (1998) 1031–1043.
[9] R.A. Dougal, S.Y. Liu, High performance micropane electron beam window, J. Vac. Sci. Technol. B 18 (2000) 2750–2756.
[10] D.Y. Lee, K. Vafai, Analytical characterization and conceptual assessment of solid and fluid temperature differentials in porous media, Int. J. Heat Mass Transfer 42 (1999) 423–435.
[11] P.X. Jiang, Z.P. Ren, Numerical investigation of forced convection heat transfer in porous media using a thermal non-equilibrium model, Int. J. Heat Fluid Flow 22 (2001) 102–110.
[12] G.P. Peterson, C.S. Chang, Two-phase heat dissipation utilizing porous-channels of high-conductivity material, J. Heat Transfer 120 (1998) 243–252.
[13] A.R. Martin, C. Saltiel, W. Shyy, Heat transfer enhancement with porous inserts in recirculating flows, J. Heat Transfer 120 (1998) 458–467.
[14] A. Amiri, K. Vafai, T.M. Kuzay, Effect of boundary conditions on non-Darcian heat transfer through porous media and experimental comparisons, Numer. Heat Transfer (A) 27 (1995) 651–664.
[15] P.X. Jiang, Z.P. Ren, B.X. Wang, Numerical simulation of forced convection heat transfer in porous plate channel using thermal equilibrium and nonthermal equilibrium models, Numer. Heat Transfer A-Applic. 35 (1999) 99–113.

[16] Guide to the Expression of Uncertainty of Measurement 1995. International Organization for Standardization, Geneva, Switzerland. ISBN 92-67-10188-9.
[17] B.V. Antohe, J.L. Lage, D.C. Price, R.M. Weber, Numerical characterization of micro-heat exchangers using experimentally tested porous aluminum layers, Int. J. Heat Fluid Flow 17 (1996) 594–603.
[18] A. Bhattacharya, V.V. Calmidi, R.L. Mahajan, Thermophysical properties of high porosity metal foam, Int. J. Heat Mass Transfer 45 (2002) 1017–1033.